



A NUMERICAL STUDY ON THE MHD TERNARY HYBRID NANOFLUID ($Cu - Al_2O_3 - TiO_2/H_2O$) IN THE PRESENCE OF THERMAL STRATIFICATION AND RADIATION ACROSS A VERTICALLY STRETCHING CYLINDER IN A POROUS MEDIUM

 Rupam Shankar Nath*,  Rudra Kanta Deka

Department of Mathematics, Gauhati University, Guwahati-781014, Assam

*Corresponding Author e-mail: rupamnath23@gmail.com

Received January 7, 2024; revised January 31, 2024; accepted February 13, 2024

The primary objective of this study is to investigate the influence of thermal stratification on the magnetohydrodynamics (MHD) flow of water-based nano, hybrid, and ternary hybrid nanofluids, as they pass a vertically stretching cylinder within a porous media. The nanoparticles Cu , Al_2O_3 , and TiO_2 are suspended in a base fluid H_2O , leading to the formation of a ternary hybrid nanofluid ($Cu + Al_2O_3 + TiO_2/H_2O$). The use of a relevant similarity variable has been utilized to simplify the boundary layer equations which control the flow and transform the coupled nonlinear partial differential equations into a collection of nonlinear ordinary differential equations. The numerical results are calculated with the 3-stage Lobatto IIIa approach, specifically implemented by Bvp4c in MATLAB. This study presents a graphical and numerical analysis of the effects of various non-dimensional parameters, such as the Prandtl number, radiation parameter, heat source/sink parameter, magnetic parameter, porosity parameter, curvature parameter, thermal stratification parameter, and thermal buoyancy parameter, on the velocity, temperature, skin-friction coefficient, and Nusselt number. The impacts of these parameters are visually depicted through graphs and quantitatively represented in tables. The ternary hybrid nanofluid has a higher heat transfer rate than the hybrid nanofluid, and the hybrid nanofluid has a higher heat transfer rate than ordinary nanofluids.

Keywords: *Thermal Stratification; Stretching Vertical Cylinder; Ternary Hybrid Nanofluid; Porous Medium; Thermal Radiation; MHD; bvp4c*

PACS: 44.05.+e, 44.25.+f, 44.27.+g, 44.40.+a, 47.11.-j, 44.30.+v

1. INTRODUCTION

Ternary hybrid nanofluids are a specific kind of fluid that is made up of three distinct kinds of nanoparticles that are scattered throughout a base fluid. This article presents a study on the ternary hybrid nanofluid composed of copper (Cu), aluminum oxide (Al_2O_3), and titanium dioxide (TiO_2) nanoparticles, which are evenly distributed inside a water-based fluid. This ternary hybrid nanofluid has unique qualities that make it suitable for a variety of applications. The presence of copper (Cu) nanoparticles into the nanofluid has been found to improve thermal conductivity, whilst the addition of aluminum oxide (Al_2O_3) and titanium dioxide (TiO_2) nanoparticles has been observed to enhance heat transfer efficiency and stability. The utilization of this nanofluid is applicable in various applications such as heat exchangers, cooling systems, and electronic devices, with the purpose of enhancing heat dissipation and improving thermal management. Copper nanoparticles are known to possess antibacterial capabilities, whereas (TiO_2) nanoparticles have photocatalytic activity against bacteria and other bacteria. The application of the ternary hybrid nanofluid, comprising $Cu - Al_2O_3 - TiO_2$, presents a promising avenue for the development of antibacterial coatings on various surfaces, including medical equipment, textiles, and food packaging. These coatings effectively impede bacterial growth and contribute to the preservation of hygiene. Titanium dioxide (TiO_2) nanoparticles have photocatalytic properties, rendering them capable of facilitating the breakdown of organic contaminants and the disinfection of water. The use of the $Cu - Al_2O_3 - TiO_2$ ternary hybrid nanofluid has potential for application in water treatment procedures, facilitating the elimination of pollutants and enhancing the overall quality of water resources.

The term "nanofluid" refers to a type of artificial fluid that is characterized by the presence of very small particles in a base fluid suspended and typically have a size of less than 100 nanometers. The concept of nanofluid, first presented by [1], proposes that heat transfer fluids with floating metallic nanoparticles could provide a revolutionary new type of heat transfer fluids. [2] and [3] investigated the natural convective flow of nanofluids with radiation for moving vertical plate and vertical channel, respectively. In both research articles, the authors explored water-based nanofluids that include titanium dioxide, aluminum oxide, and copper. In the occurrence of heat production or absorption, [4] looks for a lie group solution to the problem of how the nanofluid moves past a horizontal plate reacting chemically. [5] uses the HAM to analyze the entropy of a nanofluid

consisting of water as the primary fluid and one of four distinct kinds of nanoparticles: TiO_2 , Al_2O_3 , Cu , and CuO flowing through a stretchable permeable surface. A numerical investigation on the flow of nanofluids in the boundary layer across a moving flat plate was performed by [6] to study the impacts of thermal radiation, viscous dissipation and thermal diffusion. In the context of velocity slip and temperature leap, [7] carried out an analytical investigation on the MHD nanofluid flow for a variety of water-based nanoparticles as they passed a continually stretching/shrinking permeable sheet. [8] applied the Lattice Boltzmann method for studying the MHD Cu-water nanofluid under the presence of Lorentz forces. Furthermore, [9] conducted a research on MHD Cu-water nanofluid flow across a cone and a wedge influenced by nonlinear thermal radiation. [10] and [11] researched the impacts of heat and mass transfer on nanofluid passing a moving or fixed vertical plate in the presence of a heat source and a chemical reaction, respectively. Additionally, MHD boundary layer nanofluid flow was studied by [12] as it passed over an exponentially accelerating vertical plate in presence of thermal radiation.

[13] and [14] examined the impacts of thermal and mass stratification over a vertical wavy truncated cone and a wavy surface, respectively. Furthermore, [15] have investigated how both stratification effects affect infinite vertical cylinders. [16] and [17] conducted a study to investigate the combined impact of thermal stratification and chemical reaction on the flow past an infinite vertical plate and an accelerated vertical plate, correspondingly. Similarly, [18] looks at how thermal stratification affects unsteady parabolic flow past an infinite vertical plate. [19] investigates the thermal stratification effects of a hybrid nanofluid consisting of $Cu - Al_2O_3/H_2O$ in a porous medium. Their study focuses on a vertically stretched cylinder and considers the influence of heat sink/source. They found that the thermal conductivity of hybrid nanofluids was significantly higher than that of nanofluids. Hence, the utilization of hybrid nanofluids exhibits a significant influence on enhancing thermal advancements.

[20] aims to investigate the heat transfer characteristics of the magnetohydrodynamic Casson hybrid nanofluid in the presence of a non-Fourier heat flux model and linear thermal radiation along a horizontal porous stretched cylinder. With melting/non-melting heat transfer in mind, [21] is interested in the laminar, stable electro magnetohydrodynamic flow and entropy formation of SWCNT-blood nanofluid. The study of magneto $Cu - Al_2O_3$ /water hybrid nanofluid flow in a non-Darcy porous square cavity was done by [22].

The study conducted by [23] focuses on investigating the phenomenon of natural convection within a sinusoidal wavy cavity that is filled with a hybrid nanofluid consisting of $TiO_2 - Cu$ particles suspended in water. The analysis takes into account the influence of internal heat generation, an angled magnetic field, and thermal radiation on the convection process. The investigation conducted by [24] focused on the nonlinear buoyancy-driven flow of hybrid nanofluid passing a spinning cylinder, taking into account the effects of quadratic thermal radiation.

[25] conducted a study on the impact of non-linear Darcy-Forchheimer flow in the context of electromagnetic hydrodynamics (EMHD) ternary hybrid nanofluid, namely composed of $Cu - CNT - Ti$ and water. They found that the ternary hybrid nanofluid had a greater impact on the temperature profile than either the nanofluid or the hybrid nanofluid alone. [26] conducted a study on the heat transport characteristics of ternary hybrid nanofluid flow in the presence of a magnetic dipole with nonlinear thermal radiation. [27] performed an investigation on the computational valuation of Darcy ternary-hybrid nanofluid flow through an extending cylinder with induction effects. In order to improve the heat transfer of a magnetized ternary hybrid nanofluid $Cu - Al_2O_3 - MWCNT$ /water, [28] investigated the influence of nanoparticle shape.

The primary objective of [29] research is to investigate the application of a water-based ternary hybrid nanofluid in the context of advanced cooling for radiators. This nanofluid comprises three distinct types of nanoparticles: spherical aluminum oxide (Al_2O_3) cylindrical carbon nanotubes (CNT), and platelet-shaped particles (Graphene). [30] analyze the behavior of a ternary hybrid nanofluid (THNF) with tangent hyperbolic (T-H) flow characteristics as it interacts with a rough-yawed cylinder. The motion of the cylinder is induced using impulsive means, and the study focuses on the mixed convection mechanism in conjunction with periodic magnetohydrodynamics. The impact of suction and heat source on MHD stagnation point flow of ternary hybrid nanofluid ($Cu - Fe_3O_4 - SiO_2$ /polymer) over convectively heated stretching/shrinking cylinder has been researched by [31]. [32] conducted research on the similarity solutions of the governing equations that describe the dynamics of a colloidal mixture consisting of water, spherical carbon nanotubes, cylindrical graphene, and platelet alumina nanoparticles. The study considered various levels of partial slip and examined the cases of forced convection, free convection, and mixed convection.

According to the literature review, as was mentioned in a previous research, no one has tried to show the MHD ternary nanofluid past a Vertically Stretching Cylinder in a porous medium. The main objective of the present study is to examine the heat transfer properties of a ternary hybrid nanofluid consisting of $Cu - Al_2O_3 - TiO_2$ particles dispersed in water. This investigation focuses on the heat transfer behavior around a Vertically Stretching Cylinder, taking into account the effects of thermal stratification, thermal radiation, and uniform heat sources and sinks. The governing equations of non-linear partial differential equations (PDEs) are transformed into ordinary differential equations (ODEs) by employing suitable self-similarity variables within the `bvp4c` solver of the MATLAB software. The `Bvp4c` technique utilized in this study to simulate the problem

is widely recognized, as demonstrated by its discussion and application in MATLAB by Shampine et al., [33] and Kierzenka et al., [34]. The graphical representation of the results is provided for several parameters such as δ, M, K, R, Q, Pr and λ .

2. MATHEMATICAL ANALYSIS

Consider a two-dimensional steady in-compressible ternary hybrid nanofluid consisting of $Cu - Al_2O_3 - TiO_2/H_2O$, which is immersed in a porous medium over a vertical stretchable cylinder of radius r_0 . The system is subjected to the influence of a heat source/sink, thermal stratification and thermal radiation. The flow of the ternary hybrid nanofluid is assumed to be in the axial x -direction, with the r coordinate representing the direction normal to the x -axis, as depicted in Figure 1. In this context, the variables "u" and "v" represent the velocity components of the ternary hybrid nanofluid along the r and x - axes, respectively. In this study, a magnetic field with a magnitude of B_0 is applied in a direction perpendicular to the propagation of the ternary hybrid nanofluid. The flow issue takes into account the thermal buoyancy effect while disregarding the Joule's impact. The velocity that causes linear stretching of the vertical cylinder is denoted as $u = a \frac{x}{l}$, where 'a' and 'l' represent the velocity and characteristic length of the cylinder, respectively. $T_w(x) = T_0 + A (\frac{x}{l})$ represents the assumed temperature of the wall, while $T_\infty(x) = T_0 + B (\frac{x}{l})$ represents the temperature of the ternary hybrid nanofluid at the ambient condition, where A, B , and T_0 are non-negative constants and the starting temperature, correspondingly. The governing equations for continuity, momentum, and energy in the context of a ternary hybrid nanofluid, as presented by [19], can be expressed as follows.

$$\frac{\partial(ru)}{\partial x} + \frac{\partial(rv)}{\partial r} = 0 \tag{1}$$

$$u \frac{\partial u}{\partial x} + v \frac{\partial u}{\partial r} = \frac{\mu_{mnf}}{\rho_{mnf}} \frac{1}{r} \frac{\partial}{\partial r} \left(r \frac{\partial u}{\partial r} \right) + \frac{(\rho\beta_T)_{mnf}}{\rho_{mnf}} g(T - T_\infty) - \frac{\sigma_{mnf}}{\rho_{mnf}} B_0^2 u - \frac{\mu_{mnf}}{\rho_{mnf}} \frac{u}{k'} \tag{2}$$

$$u \frac{\partial T}{\partial x} + v \frac{\partial T}{\partial r} = \frac{k_{mnf}}{(\rho c_p)_{mnf}} \frac{1}{r} \frac{\partial}{\partial r} \left(r \frac{\partial T}{\partial r} \right) - \frac{1}{(\rho c_p)_{mnf}} \frac{1}{r} \frac{\partial}{\partial r} \left(r \frac{\partial q'_r}{\partial r} \right) + \frac{Q_0}{(\rho c_p)_{mnf}} (T - T_\infty) \tag{3}$$

The following are the boundary conditions:

$$\begin{aligned} u = a \frac{x}{l}, \quad v = 0, \quad T = T_w(x) & \quad \text{when } r = r_0 \\ u = 0, \quad T \rightarrow T_\infty(x) & \quad \text{when } r \rightarrow \infty \end{aligned}$$

The radiative heat flux q'_r in Eqn. (2) is approximated by using the Rosseland approximation [35], as the nanofluid is assumed to be an optically thick fluid. In light of the research conducted by [7], the equation (3) can be rewritten as

$$u \frac{\partial T}{\partial x} + v \frac{\partial T}{\partial r} = \frac{k_f}{(\rho c_p)_{mnf}} \left(\frac{k_{mnf}}{k_f} + \frac{16\sigma^* T_\infty^3}{3k_f k} \right) \frac{1}{r} \frac{\partial}{\partial r} \left(r \frac{\partial T}{\partial r} \right) + \frac{Q_0}{(\rho c_p)_{mnf}} (T - T_\infty)$$

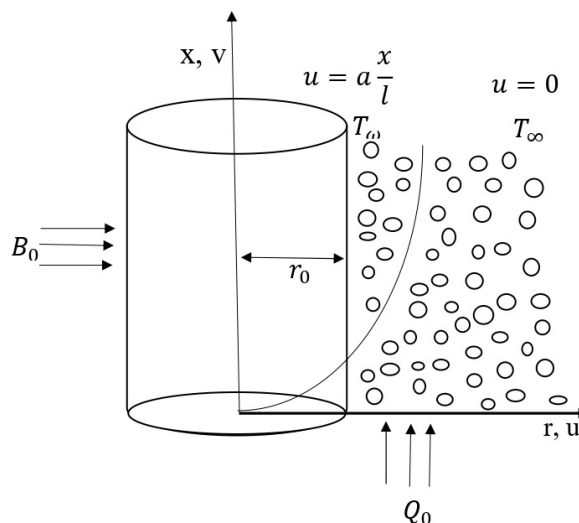


Figure 1. Physical Model and Coordinate system

The similarity transformation (Ref. [19]) used in Equations (1)-(3) are as follows

$$\eta = \frac{r^2 - r_0^2}{2r_0} \sqrt{\frac{a}{\nu_f l}}, \quad \psi = \sqrt{\frac{a\nu_f}{l}} x r_0 f(\eta), \quad \theta = \frac{T - T_\infty(x)}{T_w(x) - T_0}$$

and we provide non-dimensional quantities in the following:

$$M = \frac{l\sigma_f B_0^2}{a\rho_f}, \quad K = \frac{l\nu_f}{ak}, \quad \gamma = \sqrt{\frac{l\nu_f}{ar_0^2}}, \quad \lambda = \frac{Gr}{Re_x^2}, \quad \delta = \frac{B}{A}, \quad Q = \frac{Q_0 l}{a(\rho c_p)_f}$$

$$R = \frac{16\sigma^* T_\infty^3}{3k_f k}, \quad Pr = \frac{\nu_f(\mu c_p)_f}{k_f}$$

where, M is the magnetic parameter, K is the porosity parameter, γ is the curvature parameter, λ is the thermal buoyancy parameter, δ is the thermal stratification parameter, Q is the heat source/sink parameter, R is the radiation parameter, Pr is the Prandtl number.

The stream function ψ is introduced to satisfy continuity equation (1) in the manner that $u = \frac{1}{r} \frac{\partial \psi}{\partial r}$ and $v = -\frac{1}{r} \frac{\partial \psi}{\partial x}$. Hence, the non-dimensional forms of the transformed equations are given by

$$f'^2 - ff'' = a_1 [2\gamma f'' + (1 + 2\gamma\eta)f'''] + a_2 \lambda \theta - (a_3 M + a_1 K) f' \tag{4}$$

$$f'(\theta + \delta) - f\theta' = a_4 [2\gamma\theta' + (1 + 2\gamma\eta)\theta''] + a_5 \theta \tag{5}$$

where,

$$x_1 = \frac{\mu_{mnf}}{\mu_f}, \quad x_2 = \frac{\rho_f}{\rho_{mnf}}, \quad x_3 = \frac{(\rho\beta_T)_{mnf}}{(\rho\beta_T)_f}, \quad x_4 = \frac{(\rho C_p)_f}{(\rho C_p)_{mnf}}, \quad x_5 = \frac{\sigma_{mnf}}{\sigma_f}, \quad x_6 = \frac{k_{mnf}}{k_f}$$

$$a_1 = x_1 x_2, \quad a_2 = x_2 x_3, \quad a_3 = x_2 x_5, \quad a_4 = \frac{x_4 x_6 + R}{Pr}, \quad a_5 = Q x_4$$

Here, the symbols $\mu_{mnf}, \rho_{mnf}, (\beta_T)_{mnf}, (\rho C_p)_{mnf}, \sigma_{mnf}, k_{mnf}$ represent the ternary hybrid nanofluid's coefficient of viscosity, electrical conductivity, thermal expansion, heat capacity, density and thermal conductivity, respectively. Also, $\mu_f, \rho_f, (\beta_T)_f, (\rho C_p)_f, \sigma_f, k_f$ denote the base fluid's coefficient of viscosity, electrical conductivity, thermal expansion, heat capacity, density and thermal conductivity correspondingly.

The transformed boundary conditions are as follows :

$$\begin{array}{llll} f(\eta) = 0 & f'(\eta) = 1 & \theta(\eta) = 1 - \delta & \text{at } \eta = 0 \\ & f'(\eta) \rightarrow 0 & \theta(\eta) \rightarrow 0 & \text{as } \eta \rightarrow \infty \end{array} \tag{6}$$

The thermo-physical properties of ternary hybrid nanofluid are as follows:

$$\begin{aligned} \mu_{mnf} &= \frac{\mu_f}{(1 - \phi_1)^{2.5}(1 - \phi_2)^{2.5}(1 - \phi_3)^{2.5}} \\ \rho_{mnf} &= (1 - \phi_3) [(1 - \phi_2) \{ (1 - \phi_1)\rho_f + \phi_1\rho_{s1} \} + \phi_2\rho_{s2}] + \phi_3\rho_{s3} \\ (\rho c_p)_{mnf} &= (1 - \phi_3) [(1 - \phi_2) \{ (1 - \phi_1)(\rho c_p)_f + \phi_1(\rho c_p)_{s1} \} + \phi_2(\rho c_p)_{s2}] + \phi_3(\rho c_p)_{s3} \\ (\rho\beta_T)_{mnf} &= (1 - \phi_3) [(1 - \phi_2) \{ (1 - \phi_1)(\rho\beta_T)_f + \phi_1(\rho\beta_T)_{s1} \} + \phi_2(\rho\beta_T)_{s2}] + \phi_3(\rho\beta_T)_{s3} \\ k_{nf} &= \left[\frac{(k_{s1} + 2k_f) - 2\phi_1(k_f - k_{s1})}{(k_{s1} + 2k_f) + \phi_1(k_f - k_{s1})} \right] k_f, \quad k_{hnf} = \left[\frac{(k_{s2} + 2k_{nf}) - 2\phi_2(k_{nf} - k_{s2})}{(k_{s2} + 2k_{nf}) + \phi_2(k_{nf} - k_{s2})} \right] k_{nf} \\ k_{mnf} &= \left[\frac{(k_{s3} + 2k_{hnf}) - 2\phi_3(k_{hnf} - k_{s3})}{(k_{s3} + 2k_{hnf}) + \phi_3(k_{hnf} - k_{s3})} \right] k_{hnf}, \quad \sigma_{nf} = \left[\frac{(\sigma_{s1} + 2\sigma_f) - 2\phi_1(\sigma_f - \sigma_{s1})}{(\sigma_{s1} + 2\sigma_f) + \phi_1(\sigma_f - \sigma_{s1})} \right] \sigma_f \\ \sigma_{hnf} &= \left[\frac{(\sigma_{s2} + 2\sigma_{nf}) - 2\phi_2(\sigma_{nf} - \sigma_{s2})}{(\sigma_{s2} + 2\sigma_{nf}) + \phi_2(\sigma_{nf} - \sigma_{s2})} \right] \sigma_{nf}, \quad \sigma_{mnf} = \left[\frac{(\sigma_{s3} + 2\sigma_{hnf}) - 2\phi_3(\sigma_{hnf} - \sigma_{s3})}{(\sigma_{s3} + 2\sigma_{hnf}) + \phi_3(\sigma_{hnf} - \sigma_{s3})} \right] \sigma_{hnf} \end{aligned}$$

where ϕ_1, ϕ_2 and ϕ_3 are volume fraction of Cu (Copper), Al_2O_3 (aluminium oxide) and TiO_2 (titanium oxide) nanoparticles respectively. The suffixes mnf, hnf, nf, f, s1, s2, s3 denote ternary hybrid nanofluid, hybrid nanofluid, nanofluid, base fluid, solid nanoparticles of copper (Cu), aluminum oxide (Al_2O_3), and titanium dioxide (TiO_2) correspondingly.

The skin friction coefficient and local Nusselt number are defined by

$$C_f Re_x^{1/2} = \frac{1}{(1 - \phi_1)^{2.5}(1 - \phi_2)^{2.5}(1 - \phi_3)^{2.5}} f''(0) \quad \text{and} \quad Nu_x Re_x^{-1/2} = -\frac{k_{mnf}}{k_f} \theta'(0)$$

where, Re_x is the local Reynolds Number.

Table 1. Thermo-physical Properties of water and nanoparticles [2]

Physical Properties	H_2O (base fluid)	Cu (s1)	Al_2O_3 (s2)	TiO_2 (s3)
ρ (kg/m^3)	997.1	8933	3970	4250
C_p (J/kgK)	4179	385	765	686.2
k (W/mK)	0.613	401	40	8.9538
$\beta_t \times 10^5$ (K^{-1})	21	1.67	0.85	0.9
σ (s/m)	5.5×10^{-6}	59.6×10^6	35×10^6	2.6×10^6

3. METHOD OF SOLUTION

The `bvp4c` solver, built into the computational platform MATLAB, is used to numerically solve the system of higher-order nonlinear ODEs given by Equations (4)-(5) and the boundary conditions (6). This technique has been extensively utilized by professionals and researchers in order to solve fluid flow problems. The `bvp4c` solver, created by Jacek Kierzenka and Lawrence F. Shampine of Southern Methodist University in Texas, was introduced by Hale [36]. The `bvp4c` solver is a finite modification algorithm that uses the Lobatto IIIA implicit Runge-Kutta method to produce numerical solutions with fourth-order accuracy. This method gives the necessary accuracy when a guess is made for the initial mesh points and step-size changes. In the study conducted by Waini et al. [37], it was found that the `bvp4c` solver yielded satisfactory results in comparison to both the shooting technique and Keller box method. Here, we need to reduce the higher order derivatives with respect to η . This can be done by introducing the following new variables:

$$f = y(1), \quad f' = y(2), \quad f'' = y(3), \quad \theta = y(4), \quad \theta' = y(5)$$

$$\frac{d}{d\eta} \begin{bmatrix} y(1) \\ y(2) \\ y(3) \\ y(4) \\ y(5) \end{bmatrix} = \begin{bmatrix} y(2) \\ y(3) \\ \frac{y(2)^2 - y(1)y(3) - a_2\lambda y(4) + (a_3M + a_1K)y(2) - 2a_1\gamma y(3)}{(1+2\gamma\eta)a_1} \\ y(5) \\ \frac{y(2)(y(4)+\delta) - y(1)y(5) - 2a_4\gamma y(5) - a_5y(4)}{(1+2\gamma\eta)a_4} \end{bmatrix}$$

and boundary condition are expressed as

$$ya(1), \quad ya(2) - 1, \quad ya(4) - 1 + \delta, \quad yb(2), \quad yb(4)$$

where ya is the condition at $\eta = 0$ and yb is the condition at $\eta = \infty$

4. RESULT AND DISCUSSIONS

The numerical calculations were performed in `bvp4c` solver of MATLAB, and the outcomes are displayed in Figures (2)-(13) and Tables 3,5. Table 2 presents the absolute Skin friction Coefficient and local Nusselt Number values obtained from the current investigation, which are compared to the findings reported by Ashish et al. [19]. This comparison specifically excludes nanoparticle volume fractions of TiO_2 with $R = 0$. This study reveals that the `bvp4c` algorithm is capable of generating numerical results that are accurate and in agreement with the results obtained from alternative methods.

The following values are used in the study: $\delta = 0.2, \gamma = 0.1, M = 1.5, K = 2, R = 1, Q = 0.2, \lambda = 1.2, Pr = 6.2, \phi_1 = 0.05, \phi_2 = 0.15$ and $\phi_3 = 0.2$. The Fig. 2 displays the impact of thermal stratification(δ) parameters on the velocity $f'(\eta)$. The velocity decreases as thermal stratification(δ) increase. If the thermal stratification(δ) parameter rises, the efficient convective potential between the hot wall and the surrounding fluid drops. The buoyancy force is reduced as a result of this this, which reduces the flow velocity. As shown

Table 2. Comparison of Skin friction Coefficient and local Nusselt Number when $\phi_3 = R = 0$

Pr	M	δ	Ashish et al. $-C_f Re_x^{1/2}$	Present Study $-C_f Re_x^{1/2}$	Ashish et al. $Nu_x Re_x^{-1/2}$	Present Study $Nu_x Re_x^{-1/2}$
0.7 6.2	1.2	0.1	2.7886	2.7850	0.7266	0.7283
			2.9398	2.9297	2.7885	2.7889
	1.2	0.3	2.7076	2.6969	2.8622	2.8633
			3.0135	3.0090	2.6012	2.6044

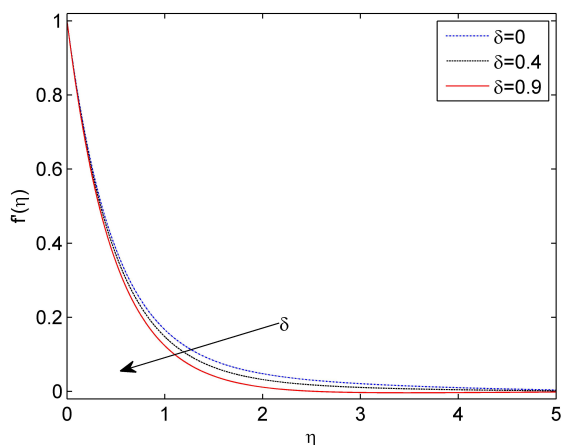


Figure 2. Effects of δ on Velocity Profile

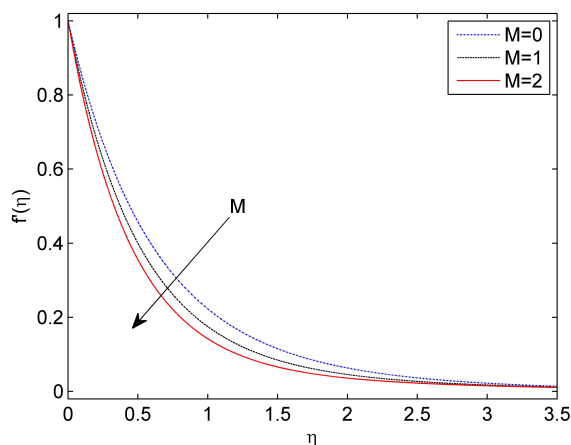


Figure 3. Effects of M on Velocity Profile

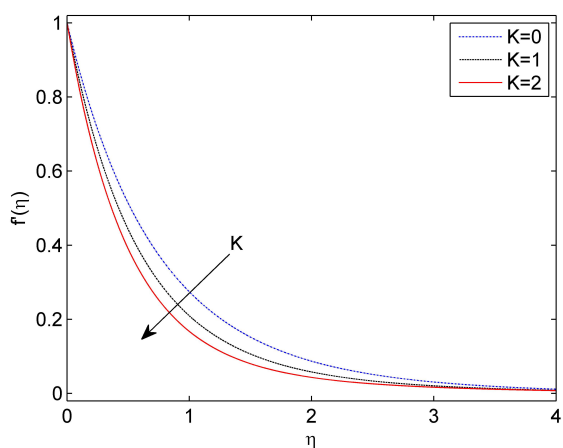


Figure 4. Effects of K on Velocity Profile

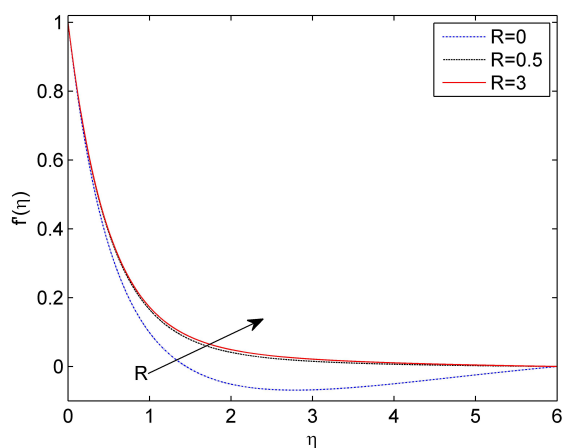


Figure 5. Effects of R on Velocity Profile

in Fig. 3, the fluid velocity $f'(\eta)$ decreases as the value of M is increased. As magnetic parameter(M) grows higher, the thickness of the momentum boundary layer shrinks. This pattern emerges because the Lorentz force produced by the horizontal magnetic field slows down the velocity of the ternary hybrid nanofluid. The impact of the porosity parameter(K) on velocity $f'(\eta)$ of the nanofluid is shown in Fig. 4. The velocity decreases as the porosity parameter value increases. The relationship between K and the diameter of the porous medium is inverse, implying that as K grows, the diameter of the porous medium decreases progressively. This reduction in diameter hinders the fluid's ability to flow through the porous medium. As a result of this obstruction, which was induced by porosity parameter(K), the velocity of the fluid dropped.

As shown in Fig. 5, as the value of R goes up, the velocity $f'(\eta)$ of the fluid goes up. With a higher value of R , the thermal conduction contribution becomes more important while the thermal radiative contribution increases. Since the radiative flux increases with increasing R , the velocity of the boundary layer of fluids increases. The effects of λ on the velocity of the fluid, is represented by Fig. 6. It is observed that the velocity will increase as the values of λ is increased. When λ is raised, the thermal buoyancy forces is made stronger. This indicates that the buoyancy forces tend to increase the velocity of the fluid.

The Fig. 7 displays that the temperature of the fluid goes down as the thermal stratification(δ) goes up. The temperature gradient between the heated wall and the surrounding fluid will decrease when the thermal stratification(δ) is present. Hence, the thermal boundary layer thickens and the temperature falls. The temperature of the fluid increases with increasing values of R in Fig. 8. This is because of the fact that higher R values indicate a higher thermal radiative flux, which ultimately results in higher temperatures. This can be seen as a manifestation of the fact that temperatures have increased.

The impact of a heat source parameter(Q) on temperature profile is seen in Fig. 9. Since the values of heat source parameter (Q) raises, the fluid temperature also increase. This characteristic matches how the fluid behaves physically in general. Fig. 10 illustrates the influence of Pr on the temperature profile of the fluid. As

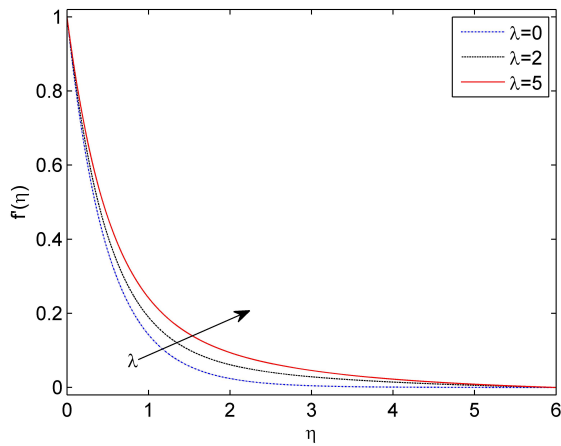


Figure 6. Effects of λ on Velocity Profile

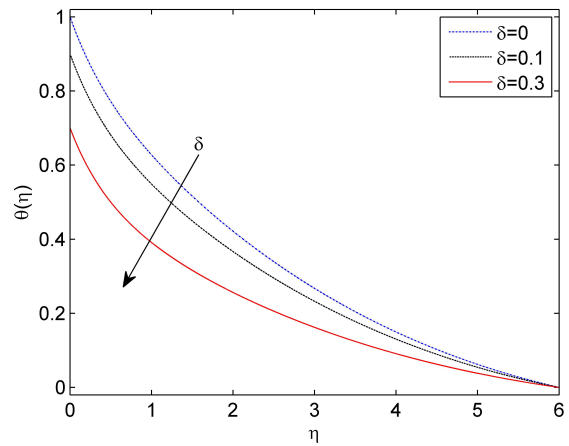


Figure 7. Effects of δ on Temperature Profile

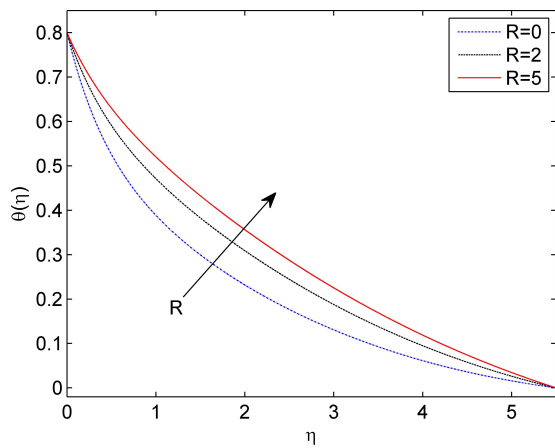


Figure 8. Effects of R on Temperature Profile

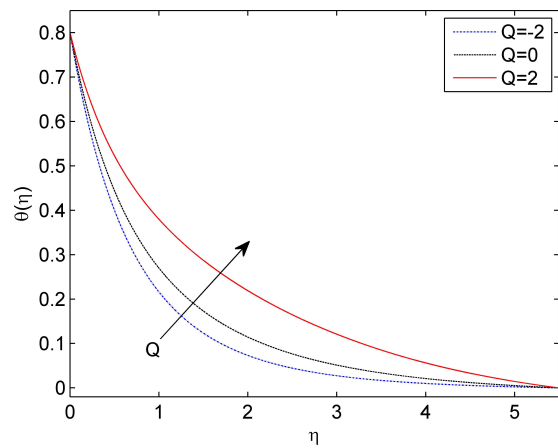


Figure 9. Effects of Q on Temperature Profile

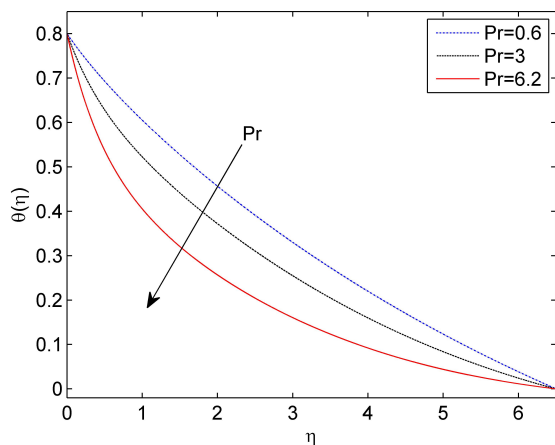


Figure 10. Effects of Pr on Temperature Profile

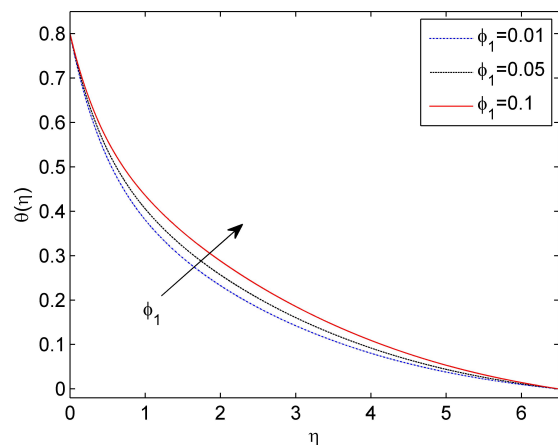


Figure 11. Effects of ϕ_1 on Temperature Profile

the Pr goes up, the temperature of the fluid goes down. It's clear that a fluid with a high Prandtl number has a low thermal conductivity. This means that heat doesn't move as easily through the fluid, so the transfer rate goes down and the thermal boundary layer gets thinner. Hence, the temperature of the fluid drops.

As the solid volume fraction of Cu nanoparticles increases, while the volume fractions of Al_2O_3 and TiO_2 remain constant, the temperature profile increases, as seen in Fig. 11. Furthermore, it can be observed from

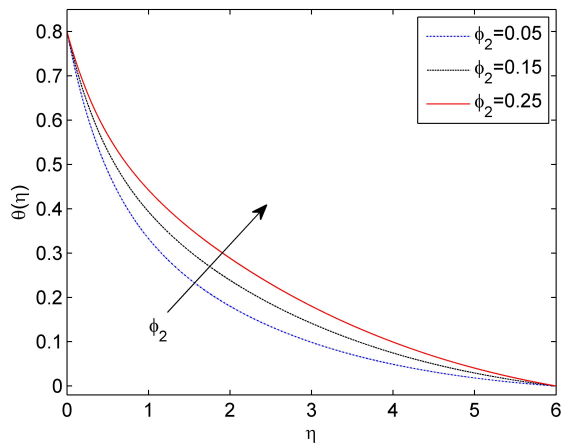


Figure 12. Effects of ϕ_2 on Temperature Profile

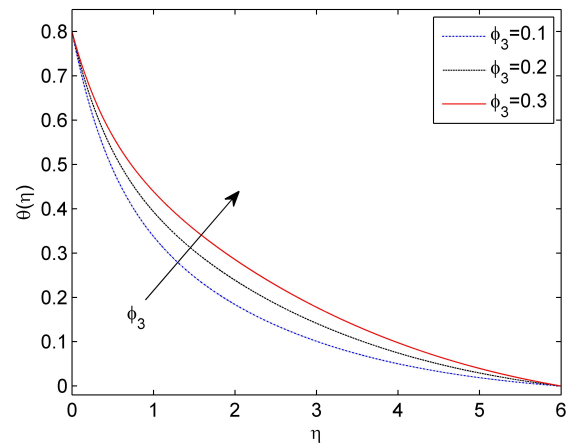


Figure 13. Effects of ϕ_3 on Temperature Profile

Fig. 12 that the temperature is increased with the increasing volume fraction of Al_2O_3 , while the volume fraction of Cu and TiO_2 remains constant. Similarly, ϕ_3 also increases the temperature profile as seen in Fig. 13.

Tables 3 present the effects on skin friction and local Nusselt number for different flow parameters. As the value of thermal stratification (δ) increases, there is a decrease in both skin friction and the local Nusselt number. An decrease in the magnitude of skin friction and Nusselt number is observed when the values of magnetic parameter(M) and porosity parameter(K) increase. The skin friction and Nusselt number exhibit an increase as the value of λ increases. For Pr , there is a decrease in skin friction while there is a rise in the Nusselt number. A decrease in the rate of heat transfer is observed as the radiation parameter (R) increases, while the opposite tendency is observed for the skin friction with an increase in R . Similarly, it can be noticed that an increase in the heat source (Q) leads to a decrease in the rate of heat transfer, although an increase in Q results in an opposite trend for the skin friction. The skin friction decreases as the curvature parameter (γ) grows, but the Nusselt number increases with an increase in the value of γ .

Table 3. Skin friction Coefficient and Local Nusselt number for different values of $\delta, M, K, \lambda, Pr, R, Q, \gamma$

δ	M	K	λ	Pr	R	Q	γ	Skin-friction Coefficient	Local Nusselt Number
0								-6.0075	2.0495
0.1	1.5	2	1.2	6.2	1	0.2	0.1	-6.0465	2.0140
0.3								-6.1272	1.9747
0.2	0	2	1.2	6.2	1	0.2	0.1	-4.8297	2.4280
	0.5							-5.2804	2.2742
	1.2							-5.8562	2.0760
0.2	1.5	0	1.2	6.2	1	0.2	0.1	-4.4138	2.5682
		1						-5.3132	2.2630
		2						-6.0870	1.9962
0.2	1.5	2	0	6.2	1	0.2	0.1	-6.3426	1.7157
			1.5					-6.0270	2.0411
			3					-5.7398	2.2105
0.2	1.5	2	1.2	0.6	1	0.2	0.1	-6.0352	0.6625
				3				-6.0567	1.2203
				6.2				-6.0870	1.9962
0.2	1.5	2	1.2	6.2	0	0.2	0.1	-6.1139	2.6133
					0.5			-6.0960	2.2254
					2			-6.0750	1.6861
0.2	1.5	2	1.2	6.2	1	-0.2	0.1	-6.1368	3.0531
						0		-6.1209	2.6547
						0.2		-6.0870	1.9962
0.2	1.5	2	1.2	6.2	1	0.2	0	-5.9506	1.9767
							0.1	-6.0870	1.9962
							0.2	-6.2286	2.1174

The absolute skin friction ($-C_f Re_x^{1/2}$) and local nusselt number ($Nu_x Re_x^{-1/2}$) of nanofluid, hybrid nanofluid, and ternary hybrid nanofluid are compared in tables 4 and 5. The absolute value of skin friction of the ($Cu - Al_2O_3 - TiO_3/H_2O$) ternary hybrid nanofluid shows a significant improvement of up to 174% in comparison to the (Cu/H_2O) nanofluid. Additionally, it has been found that the difference between ternary hybrid nanofluid and common nanofluid reduces with thermal stratification(δ) for $-C_f Re_x^{1/2}$. The Nusselt Number of the ternary hybrid nanofluid displays a significant enhancement of up to 32% when compared to the conventional nanofluid. In addition, it has been discovered that thermal stratification(δ) increases the difference between ternary hybrid nanofluid and regular nanofluid for $Nu_x Re_x^{-1/2}$.

Table 4. Comparison of $-C_f Re_x^{1/2}$

δ	Cu Nanofluid	$Cu - Al_2O_3$ Hybrid Nanofluid	$Cu - Al_2O_3 - TiO_3$ Ternary Hybrid Nanofluid	Change in %
0	2.1858	3.4001	6.0075	174.8
0.1	2.2290	3.4416	6.0465	171.2
0.2	2.2747	3.4800	6.0870	167.6
0.3	2.3186	3.5245	6.1272	164.3



Table 5. Comparison of Local Nusselt Number

δ	Cu Nanofluid	$Cu - Al_2O_3$ Hybrid Nanofluid	$Cu - Al_2O_3 - TiO_3$ Ternary Hybrid Nanofluid	Change in %
0	1.6333	1.9355	2.0495	25.8
0.1	1.5823	1.8842	2.0140	27.3
0.2	1.5419	1.8095	1.9962	29.5
0.3	1.4926	1.7798	1.9747	32.3

5. CONCLUSION

The impact of thermal stratification on the flow of a ternary hybrid nanofluid ($Cu - Al_2O_3 - TiO_3/H_2O$) with magnetohydrodynamics (MHD) properties along a vertical stretchable cylinder has been studied. This investigation takes into consideration the presence of a thermal bouncy effect, thermal radiation, and heat source/sink inside a porous medium. In addition, the analysis takes into account the flow characteristics and their impact on the velocity and temperature profiles, skin friction, and local Nusselt number. The velocity profile reveals a declining tendency when the parameters δ, M and K are increased, whereas it exhibits an ascending trend with higher values of R and λ . The temperature exhibits a decrease as the magnitudes of δ and Pr increase, while it exhibits an increase with the increase of R and Q . The skin friction exhibits an increase with respect to the parameters λ, R , and Q , but it experiences a decrease in relation to the factors δ, M, K, Pr and γ . An upward trend in the local Nusselt number is noted as the values of λ, Pr , and γ grow, whereas it exhibits a downward trend with increasing values of δ, M, K, R and Q . The ternary hybrid nanofluid exhibits a higher magnitude of absolute skin friction ($-C_f Re_x^{1/2}$) in comparison to the hybrid nanofluid. Similarly, the absolute skin friction of hybrid nanofluids exhibits a higher value when compared to that of conventional nanofluids. The ternary hybrid nanofluid demonstrates a superior heat transfer rate in contrast to the hybrid nanofluid, whereas the hybrid nanofluid displays a higher heat transfer rate in comparison to conventional nanofluids.

ORCID

 **Rupam Shankar Nath**, <https://orcid.org/0009-0002-2352-0538>;  **Rudra Kanta Deka**, <https://orcid.org/0009-0007-1573-4890>

REFERENCES

- [1] S.U.S. Choi, and J.A. Eastman, *Enhancing thermal conductivity of fluids with nanoparticles*, Technical report, (Argonne National Lab. Argonne, IL, United States, 1995).
- [2] S. Das, and R.N. Jana, "Natural convective magneto-nanofluid flow and radiative heat transfer past a moving vertical plate," *Alexandria Engineering Journal*, **54**(1), 55-64 (2015). <https://doi.org/10.1016/j.aej.2015.01.001>
- [3] S. Das, R.N. Jana, and O.D. Makinde, "Transient natural convection in a vertical channel filled with nanofluids in the presence of thermal radiation," *Alexandria Engineering Journal*, **55**(1), 253-262 (2016). <https://doi.org/10.1016/j.aej.2015.10.013>

- [4] M.M. Rashidi, E. Momoniat, M. Ferdows, and A. Basiriparsa, "Lie group solution for free convective flow of a nanofluid past a chemically reacting horizontal plate in a porous media," *Mathematical Problems in Engineering*, **2014**, 239082 2014. <https://doi.org/10.1155/2014/239082>
- [5] M.H. Abolbashari, N. Freidoonimehr, F. Nazari, and M.M. Rashidi, "Entropy analysis for an unsteady mhd flow past a stretching permeable surface in nano-fluid," *Powder Technology*, **267**, 256–267 2014. <https://doi.org/10.1016/j.powtec.2014.07.028>
- [6] T.G. Motsumi, and O.D. Makinde, "Effects of thermal radiation and viscous dissipation on boundary layer flow of nanofluids over a permeable moving flat plate," *Physica Scripta*, **86**(4), 045003 (2012). <https://doi.org/10.1088/0031-8949/86/04/045003>
- [7] M. Turkyilmazoglu, "Exact analytical solutions for heat and mass transfer of mhd slip flow in nanofluids," *Chemical Engineering Science*, **84**, 182–187 (2012). <https://doi.org/10.1016/j.ces.2012.08.029>
- [8] M. Sheikholeslami, M.G. Bandy, R. Ellahi, and A. Zeeshan, "Simulation of mhd cu–water nanofluid flow and convective heat transfer considering lorentz forces," *Journal of Magnetism and Magnetic Materials*, **369**, 69–80 (2014). <https://doi.org/10.1016/j.jmmm.2014.06.017>
- [9] N. Sandeep, and M.G. Reddy, "Heat transfer of nonlinear radiative magnetohydrodynamic cu-water nanofluid flow over two different geometries," *Journal of Molecular Liquids*, **225**, 87–94 (2017). <https://doi.org/10.1016/j.molliq.2016.11.026>
- [10] P.C. Reddy, M.C. Raju, and G.S.S. Raju, "Free convective heat and mass transfer flow of heat-generating nanofluid past a vertical moving porous plate in a conducting field," *Special Topics and Reviews in Porous Media: An International Journal*, **7**(2), 161–180 (2016). <https://doi.org/10.1615/SpecialTopicsRevPorousMedia.2016016973>
- [11] B. Mahanthesh, B.J. Gireesha, and R.S.R. Gorla, "Heat and mass transfer effects on the mixed convective flow of chemically reacting nanofluid past a moving/stationary vertical plate," *Alexandria engineering journal*, **55**(1), 569–581 (2016). <https://doi.org/10.1016/j.aej.2016.01.022>
- [12] S.P. Jeevandhar, V. Kedla, N. Gullapalli, and S.K. Thavada, "Natural convective effects on mhd boundary layer nanofluid flow over an exponentially accelerating vertical plate," *Biointerface Research in Applied Chemistry*, **11**(6), 13790–13805 (2021). <https://doi.org/10.33263/BRIAC116.1379013805>
- [13] C.-Y. Cheng, "Double-diffusive natural convection along a vertical wavy truncated cone in non-newtonian fluid saturated porous media with thermal and mass stratification," *International Communications in Heat and Mass Transfer*, **35**(8), 985–990 (2008). <https://doi.org/10.1016/j.icheatmasstransfer.2008.04.007>
- [14] C.-Y. Cheng, "Combined heat and mass transfer in natural convection flow from a vertical wavy surface in a power-law fluid saturated porous medium with thermal and mass stratification," *International Communications in Heat and Mass Transfer*, **36**(4), 351–356 (2009). <https://doi.org/10.1016/j.icheatmasstransfer.2009.01.003>
- [15] A. Paul, and R.K. Deka, et al., "Unsteady natural convection flow past an infinite cylinder with thermal and mass stratification," *Int. J. Eng. Math.* **2017**, 8410691 (2017). <https://doi.org/10.1155/2017/8410691>
- [16] R.S. Nath, and R.K. Deka, "The effect of thermal stratification on flow past an infinite vertical plate in presence of chemical reaction," *East European Journal of Physics*, **3**, 223–232 (2023). <https://doi.org/10.26565/2312-4334-2023-3-19>
- [17] N. Kalita, R.K. Deka, and R.S. Nath, "Unsteady flow past an accelerated vertical plate with variable temperature in presence of thermal stratification and chemical reaction," *East European Journal of Physics*, **3**, 441–450 (2023). <https://doi.org/10.26565/2312-4334-2023-3-49>
- [18] R.S. Nath, R.K. Deka, and H. Kumar, "The Effect of Thermal Stratification on Unsteady Parabolic Flow past an Infinite Vertical Plate with Chemical Reaction," *East European Journal of Physics*, **4**, 77–86 (2023) <https://doi.org/10.26565/2312-4334-2023-4-08>
- [19] A. Paul, J.M. Nath, and T.K. Das, "An investigation of the MHD Cu-Al₂O/H₂O hybrid-nanofluid in a porous medium across a vertically stretching cylinder incorporating thermal stratification impact," *Journal of Thermal Engineering*, **9**(3), 799–810 (2023). <https://doi.org/10.18186/thermal.1300847>
- [20] N. Shanmugapriyan, and S. Jakeer, "Biomedical aspects of entropy generation on MHD flow of TiO₂-Ag/blood hybrid nanofluid in a porous cylinder," *Computer Methods in Biomechanics and Biomedical Engineering*, **14**, 1–18 (2023). <https://doi.org/10.1080/10255842.2023.2245520>
- [21] S. Suneetha, L. Wahidunnisa, S.R.R. Reddy, and P.B.A. Reddy, "Entropy generation on the variable electric field and emhd swcnt-blood nanofluid with melting/non-melting heat transfer," *Proceedings of the Institution of Mechanical Engineers, Part E: Journal of Process Mechanical Engineering*, **237**(6), 2314–2322 (2022). <https://doi.org/10.1177/09544089221140223>
- [22] S. Jakeer, P.B.A. Reddy, A.M. Rashad, and H.A. Nabwey, "Impact of heated obstacle position on magneto-hybrid nanofluid flow in a lid-driven porous cavity with Cattaneo-Christov heat flux pattern," *Alexandria Engineering Journal*, **60**(1), 821–835 (2021). <https://doi.org/10.1016/j.aej.2020.10.011>
- [23] J. Shaik, B.A.R. Polu, M.M. Ahmed, and R.A. Mohamed, "Characteristics of moving hot block and non-fourier heat flux model on sinusoidal wavy cavity filled with hybrid nanofluid," *The European Physical Journal Plus*, **137**(1), 131 (2022). <https://doi.org/10.1140/epjp/s13360-022-02361-y>

- [24] P. Rana, and A. Kumar, "Nonlinear buoyancy driven flow of hybrid nanofluid past a spinning cylinder with quadratic thermal radiation," *International Communications in Heat and Mass Transfer*, **139**, 106439 (2022). <https://doi.org/10.1016/j.icheatmasstransfer.2022.106439>
- [25] S. Jakeer, S.R.R. Reddy, A.M. Rashad, M.L. Rupa, and C. Manjula, "Nonlinear analysis of Darcy-Forchheimer flow in EMHD ternary hybrid nanofluid (Cu-CNT-Ti/water) with radiation effect," *Forces in Mechanics*, **10**, 100177 (2023). <https://doi.org/10.1016/j.finmec.2023.100177>
- [26] S. Nasir, S. Sirisubtawee, P. Juntharee, A.S. Berrouk, S. Mukhtar, and T. Gul, "Heat transport study of ternary hybrid nanofluid flow under magnetic dipole together with nonlinear thermal radiation," *Applied Nanoscience*, **12**(9), 2777–2788 (2022). <https://doi.org/10.1007/s13204-022-02583-7>
- [27] K.A.M. Alharbi, A.El-Sayed Ahmed, M.O. Sidi, N.A. Ahammad, A. Mohamed, M.A. El-Shorbagy, et al., "Computational valuation of Darcy ternary-hybrid nanofluid flow across an extending cylinder with induction effects," *Micromachines*, **13**(4), 588 (2022). <https://doi.org/10.3390/mi13040588>
- [28] M. Shanmugapriya, R. Sundareswaran, P.S. Kumar, and G. Rangasamy, "Impact of nanoparticle shape in enhancing heat transfer of magnetized ternary hybrid nanofluid," *Sustainable Energy Technologies and Assessments*, **53**, 102700 (2022). <https://doi.org/10.1016/j.seta.2022.102700>
- [29] M. Arif, P. Kumam, W. Kumam, and Z. Mostafa, "Heat transfer analysis of radiator using different shaped nanoparticles water-based ternary hybrid nanofluid with applications: A fractional model," *Case Studies in Thermal Engineering*, **31**, 101837 (2022). <https://doi.org/10.1016/j.csite.2022.101837>
- [30] P.M. Patil, B. Goudar, and M.A. Sheremet, "Tangent hyperbolic ternary hybrid nanofluid flow over a rough-yawed cylinder due to impulsive motion," *Journal of Taibah University for Science*, **17**(1), 2199664 (2023). <https://doi.org/10.1080/16583655.2023.2199664>
- [31] Z. Mahmood, Z. Iqbal, M.A. Alyami, B. Alqahtani, M.F. Yassen, and U. Khan, "Influence of suction and heat source on mhd stagnation point flow of ternary hybrid nanofluid over convectively heated stretching/shrinking cylinder," *Advances in Mechanical Engineering*, **14**(9), (2022). <https://doi.org/10.1177/16878132221126278>
- [32] W. Cao, I. Animasaun, S.-J. Yook, V.A. Oladipupo, and X. Ji, "Simulation of the dynamics of colloidal mixture of water with various nanoparticles at different levels of partial slip: Ternary-hybrid nanofluid," *International Communications in Heat and Mass Transfer*, **135**, 106069 (2022). <https://doi.org/10.1016/j.icheatmasstransfer.2022.106069>
- [33] L.F. Shampine, J. Kierzenka, and M.W. Reichelt, *Solving boundary value problems for ordinary differential equations in Matlab with bvp4c. Tutorial notes*, (2000). https://classes.engineering.wustl.edu/che512/bvp_paper.pdf
- [34] J. Kierzenka, and L.F. Shampine, "A bvp solver based on residual control and the Matlab pse," *ACM Transactions on Mathematical Software*, **27**(3), 299–316 (2001). <https://doi.org/10.1145/502800.502801>
- [35] S Rosseland, *Astrophysik und atom-theoretische Grundlagen*, (Springer-Verlag, Berlin, 1931).
- [36] N.P. Hale, *A sixth-order extension to the matlab bvp4c software of j. kierzenka and l. shampine*, (Department of Mathematics, Imperial College London, 2006).
- [37] I. Waini, A. Ishak, and I. Pop, "Mixed convection flow over an exponentially stretching/shrinking vertical surface in a hybrid nanofluid," *Alexandria Engineering Journal*, **59**(3), 1881–1891 (2020). <https://doi.org/10.1016/j.aej.2020.05.030>

ЧИСЕЛЬНЕ ДОСЛІДЖЕННЯ ПОТРІЙНОЇ ГІБРИДНОЇ МГД НАНОРІДИНИ ($Cu - Al_2O_3 - TiO_2/H_2O$) ЗА НАЯВНОСТІ ТЕПЛОВОЇ СТРАТИФІКАЦІЇ ТА ВИПРОМІНЮВАННЯ ЧЕРЕЗ ВЕРТИКАЛЬНО РОЗТЯГНУТИЙ ЦИЛІНДР У ПОРИСТОМУ СЕРЕДОВИЩІ

Рупам Шанкар Нат, Рудра Канта Дека

Факультет математики, Університет Гаухаті, Гувахаті-781014, Ассам

Основною метою цього дослідження є дослідження впливу термічної стратифікації на магнітогідродинамічний (МГД) потік нано-, гібридних і потрійних гібридних нанофлюїдів на водній основі, коли вони проходять повз вертикально розтягнутий циліндр у пористому середовищі. Наночастинки Cu , Al_2O_3 і TiO_2 суспендовані в базовій рідині H_2O , що призводить до утворення потрійної гібридної нанорідини ($Cu + Al_2O_3 + TiO_2/H_2O$). Використання відповідної змінної подібності було використано для спрощення рівнянь граничного шару, які керують потоком і перетворюють пов'язані нелінійні диференціальні рівняння в частинних похідних у набір нелінійних звичайних диференціальних рівнянь. Числові результати обчислюються за допомогою 3-етапного підходу Lobatto Ша, спеціально реалізованого Bvp4c у MATLAB. У цьому дослідженні представлено графічний і числовий аналіз впливу різних безрозмірних параметрів, таких як число Прандтля, параметр випромінювання, параметр джерела тепла/стоку, магнітний параметр, параметр пористості, параметр кривизни, параметр термічної стратифікації та параметр теплової плавучості, від швидкості, температури, коефіцієнта поверхневого тертя та числа Нуссельта. Вплив цих параметрів візуально зображено на графіках і кількісно представлено в таблицях. Потрійна гібридна нанофлюїд має вищу швидкість теплопередачі, ніж гібридна нанофлюїд, а гібридна нанофлюїд має вищу швидкість теплопередачі, ніж звичайні нанофлюїди.

Ключові слова: термічна стратифікація; вертикальний циліндр, що розтягується; тернарний гібридний нанофлюїд; пористе середовище; теплове випромінювання; МГД; bvp4c